Blade Deflection Measurements of a Full-Scale UH-60A Rotor System

Lawrence E. Olson
Aerospace Engineer
Larry.Olson@nasa.gov

Anita I. Abrego
Aerospace Engineer
Anita.I.Abrego@nasa.gov

NASA Ames Research Center
Moffett Field, California

Danny A. Barrows
Aerospace Engineer
Danny.A.Barrows@nasa.gov
NASA Langley Research Center
Hampton, Virginia

Alpheus W. Burner
Aerospace Engineer
Alpheus.W.Burner@nasa.gov
Jacobs Technology (ROME Group)
Hampton, Virginia

ABSTRACT

Blade deflection (BD) measurements using stereo photogrammetry have been made during the individual blade control (IBC) testing of a UH-60A 4-bladed rotor system in the 40- by 80-foot test section of the National Full-Scale Aerodynamic Complex (NFAC). Measurements were made in quadrants one and two, encompassing advance ratios from 0.15 to 0.40, thrust coefficient/solidities from 0.05 to 0.12 and rotor-system drive shaft angles from 0.0 to -9.6 deg. The experiment represents a significant step toward providing benchmark databases to be utilized by theoreticians in the development and validation of rotorcraft prediction techniques. In addition to describing the stereo measurement technique and reporting on preliminary measurements made to date, the intent of this paper is to encourage feedback from the rotorcraft community concerning continued analysis of acquired data and to solicit suggestions for improved test technique and areas of emphasis for measurements in the upcoming UH-60A Airloads test at the NFAC.

NOTATION

Airloads	refers to planned calendar year 2010 testing of a UH-60A rotor system in the NFAC
Airloads flight tests	Research flight testing of UH-60A rotor system completed in 1994 (Ref. 1)
BD system	NASA Ames/Langley blade deflection measurement system
blade azimuth	azmuthal position of a blade, deg
blade number	number assigned to a blade with blade one installed at a nominal hub azimuth of zero deg, blade two at 90 deg, etc.
BMS	blade measurement system used in Airloads flight test and IBC test to measure blade flap, lag and pitch
centroidable target	a retro-reflective target in an image whose center can be accurately determined in pixel space
DNW	Dutch-German Wind Tunnel
HART II	Higher Harmonic Control Aeroacoustic Rotor Test
IBC	individual blade control test program
image set	group of simultaneously acquired images, one image from each camera
LRTA	large rotor test apparatus
NFAC	National Full-Scale Aerodynamic Complex
SMART	Smart Material Actuated Rotor Technology
C_T	rotor system thrust coefficient, parallel to axis of drive shaft
q	dynamic pressure, lb/ft^2
V	test-section flow velocity, kts
(X,Y,Z)	wind-tunnel coordinate system with the origin at the rotor hub, X positive downstream, Y positive to starboard and Z positive up
α_s	rotor shaft angle measured from vertical, positive aft, deg
μ	advance ratio = tip velocity/V
σ	rotor system solidity = total area of blades/total area of rotor disk
Ψ	azimuth, angular position of the rotor hub measured counter clockwise, zero in the plane downstream from the rotor hub, deg

INTRODUCTION

The accurate prediction of rotor blade static and elastic deflections is a key goal in the development of improved rotorcraft design and analysis techniques. Continued progress toward more tightly coupled multi-disciplinary, high fidelity rotorcraft aeromechanics analysis techniques will be paced in part by the availability of improved and

Presented at the American Helicopter Society Aeromechanics Specialist' Conference, San Francisco, California, January 20-22, 2010.

detailed experimental measurements obtained under conditions representative of actual flight conditions. High-quality rotor blade deflection data sets are relatively rare. In 2001, photogrammetric mappings of blade deflections were obtained during the HART II rotor test at the German-Dutch Wind Tunnel (DNW) as described in reference 2. Recently, blade deflection measurements were obtained during the Smart Material Actuated Rotor Technology (SMART) test in the 40- by 80-Foot Wind Tunnel at NASA Ames Research Center (Fig. 1). This experiment measured deflections of a single rotor blade using two cameras acquiring image pairs in quadrant I (Ref. 3). The test provided the initial opportunity for BD system trouble shooting and testing and the operational experience needed to improve data acquisition and image processing techniques.

Figure 1. Boeing/DARPA SMART Rotor Test in NFAC.

The experiment discussed in the present paper is the second in the sequence of three rotor wind-tunnel tests that seek to provide a new benchmark for blade deflection data. The IBC test, conducted in the National Full-Scale Aerodynamic Complex (NFAC) 40- by 80-Foot Wind Tunnel is shown in Fig. 2. Blade deflection measurements were acquired for two rotor blades with four cameras acquiring sequences of image pairs spanning two rotor quadrants.

The third experiment, to be conducted in the same facility in 2010, is the UH-60A Airloads test. In an effort to document blade-to-blade dissimilarities, stereo photogrammetry will be applied to all four blades, for all four rotor quadrants, with an eight camera measurement system.

Figure 2. UH-60A installed on the LRTA in 40-ft by 80-foot test section of the NFAC.

APPROACH

The test equipment and experimental technique used to obtain blade deflection measurements can be summarized as follows.

Image Acquisition System

The experimental technique employs digital photogrammetry wherein two cameras (or three, in some unique azimuthal positions where a blade can be viewed with three cameras) view each rotor quadrant. For the IBC test, a total of four cameras captured time-synchronized image sets for the two downstream rotor quadrants (Fig. 3), quadrant I ($0 < \Psi < 90$ deg) and quadrant IV ($270 < \Psi < 360$ deg). These four cameras, two per quadrant, were installed in the test-section wall cavities and can be seen in figure 4. The cameras were aimed upward through windows, toward the quadrant of interest.

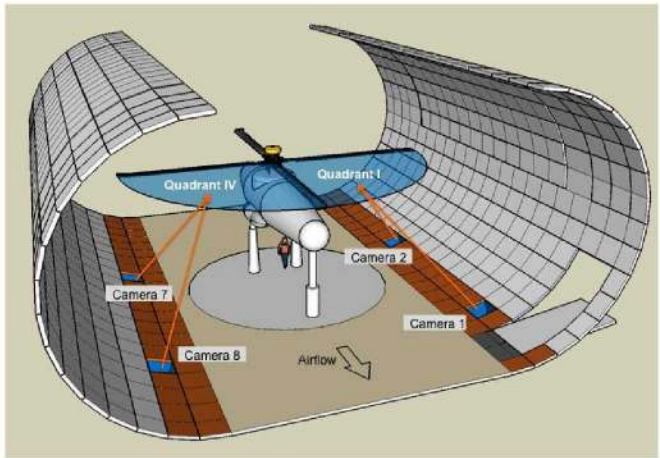

Figure 3. 40-ft by 80-foot test section schematic showing camera cavity locations for the two quadrant photogrammetry measurements.

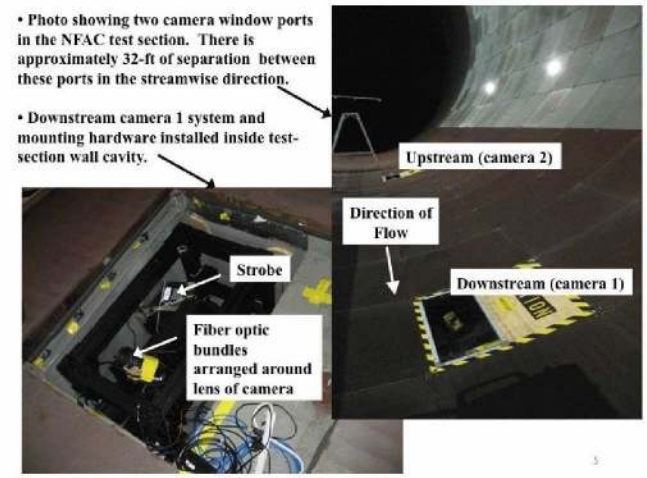

Figure 4. Installation of starboard-side camera systems in the walls of the test section.

Target illumination was provided by PerkinElmer Machine Vision 7060-10 Strobes which have high-power xenon flash lamps with a 1/3-peak pulse duration of 10 microseconds. Two strobes and one camera were located in each wall cavity. Fiber optic bundles were used to position the light sources as close as possible to the optical axes of the camera lenses. The strobes and cameras were synchronized and triggered with respect to blade azimuth location, with the strobe pulses occurring within the integration time of the simultaneously triggered 4-mega pixel CCD cameras.

The lower surface of two rotor blades was prepared with fifty, 2-inch diameter, retro-reflective targets. The targets were cut from 3M Scotchlite 7610 high reflectance adhesive tape. Figure 5 shows a targeted rotor blade with a target spanwise spacing of approximately 0.05R, and three targets per station distributed in the chordwise direction.

Figure 5. Blade with two-inch diameter retro reflective targets installed.

The data acquisition and reduction software were primarily developed at NASA. Two desktop PCs (one servicing the two cameras aimed at quadrant I and one servicing the two cameras aimed at quadrant IV) running Windows XP Professional were used for image data acquisition during IBC testing (four PCs will be used in the 4-quadrant system for the planned Airloads test). WingViewer (Ref. 4) acquisition software enables the simultaneous grab of sequences of image pairs (one sequence of pairs per PC) upon triggering from a Rotor Azimuth Synchronization Program (RASP) USB box (Ref. 5) at a given azimuth. The acquisition software provides for convenient storage to hard-disc of image pairs at each revolution of the rotor for a user-specified number of revolutions.

Data at a given azimuth were acquired by phase locking with the rotor shaft encoder. Image pairs for each quadrant were acquired once per rotor revolution, every 0.23 seconds at 258 rpm for the IBC test. At each test condition (defined for example by a unique combination of rotor thrust, advance ratio and angle of attack) image sets were acquired at a sequence of rotor system azimuth locations. For most test conditions data were acquired every 15 deg, capturing blades 1 and 2 as they pass through quadrants I and IV. Limited amounts of data were also obtained with blades at 105 and 255 deg azimuth. The number of image sets acquired at a given data point could be adjusted by the experimenter to improve the precision of ensemble averages (e.g., lag, flap and twist distributions). In general, the blade stations exhibiting the most dynamic rev-to-rev deformation variation determine the number of image sets that should be obtained. For example, a complete IBC test condition generally comprised of an ensemble average of 15 revolutions of data at 12 rotor system azimuths, producing 720 individual images. The time required to acquire the 15 image sets at each rotor azimuth was approximately 3.5 seconds for a total data acquisition time of 42 sec for the azimuth sweep. Approximately 63,000 8MB images were acquired during IBC hover and forward flight testing. In part because of the requirement to acquire image sets covering all four quadrants during the planned Airloads test, data acquisition time is expected to present more of a challenge than was the case during the IBC test. For example, a complete Airloads test condition could comprise an ensemble average of 50 revolutions of data, 8 cameras, 24 discrete rotor system azimuths, producing 9600 individual images. The time required to acquire the 50 image sets at each rotor azimuth is about 12 seconds, leading to a total data acquisition time for this particular example of approximately 5 minutes. Reducing the number of azimuthal settings and images per azimuth will proportionally reduce the acquisition time. For instance, acquiring 15 images at each of 15 azimuths would take less than 1 minute.

Accuracy Requirements and Transformation of Image Data into the Rotor Coordinate System

In an effort to insure that the measurements will be useful to analysts, the accuracy goal for photogrammetry results are tight, 0.1 deg for the instantaneous measurement of blade twist at each radial station. This blade twist measurement accuracy requirement requires that, for the UH-60A rotor, the relative location of adjacent targets at a given radial

station be located, in the rotor coordinated system, to within 0.020 inches.

Transforming the information contained in the stereo digital images into displacement of an elastic blade in the shaft coordinate system is dependent on three independent calibrations: (1) an interior calibration of the cameras (lens parameters), (2) an exterior calibration of the cameras (camera locations and pointing angles), and (3) an independent measurement of the targets on the blades relative to the local airfoil chordline. The interior calibrations and initial blade target measurements were done prior to the start of IBC testing. However, two blade target location calibrations were also obtained during IBC testing, primarily because dirty or damaged targets needed to be replaced. The exterior camera calibrations are determined as part of the post-test image analysis using known test-section ceiling target (Fig. 6) locations that were measured prior to the start of IBC testing.

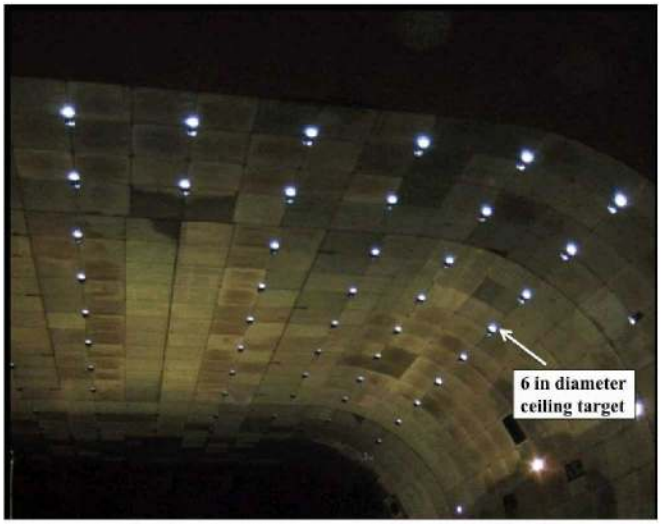

Figure 6. Ceiling of the test section with six-inch diameter targets installed.

Pre-test interior calibrations of each 4-mega pixel, 12-bit gray scale camera are performed to account for lens distortion effects and determine photogrammetric principal point and distance and the point of symmetry for distortion. The distortion parameters were determined using a 19-inch by 24-inch precision calibrated plate targeted with 121 0.5-inch diameter retro-reflective targets, whereas the photogrammetric principal point and point of symmetry for distortion were determined with a laser alignment technique (Ref. 6).

Exterior calibration of the cameras, which determines the location and orientation of each camera relative to the test section, relies on a known constellation of 84 six-inch diameter retro-reflective targets distributed over the test-section ceiling (Fig. 6). These target are distributed approximately uniformly with a nominal target-to-target spacing of 96 inches. Well over half, 48, of these targets are located on large overhead clamshell test-section doors. The relative locations of these ceiling targets are determined using the Geodetic Systems Inc. (GSI) V-STARS photogrammetric measurement system (Ref. 7) with a standard deviation of less than 0.04 inches. These measurements are combined with known global test-section geometry characteristics (flat ceiling, test-section diffusion angle (0.1 deg) and centerline and cross-stream reference points) to establish the location of the targets in the wind-tunnel coordinate system. This coordinate system is aligned with the centerline axis of the test section, and centered streamwise over the turntable upon which the large rotor test apparatus (LRTA) is mounted. In the IBC BD test data analysis, these calibrations have not been corrected for possible distortion caused by changes in test-section shell temperature or for changes potentially caused by opening and closing the 80-ton clamshell doors.

Transformation of measured target locations, blade pitch, etc. from the wind-tunnel coordinate system into the rotor coordinate system requires knowledge of the orientation and location of the rotor system hub. This transformation can be made, at least to the first order, based on the calibrated shaft encoder measurements from the NFAC data system along with measured model support and rotor test stand (e.g. LRTA) geometry. A cautionary note must be made that, if the dynamic motion of the rotor shaft in the plane of the rotor is sufficiently large, it may be more appropriate to compute the instantaneously measured target locations relative to the instantaneous position of the shaft. In a preliminary effort to measure the instantaneous position of the shaft with each image set, a ring of retro-reflective targets was installed on the instrumentation pod, located directly above the rotor hub, Fig. 7. This instrumentation pod, rigidly mounted on the axis of the rotor shaft, spinning with the rotor, should accurately track the dynamic motions of the rotor hub. Multiple projections of lines orthogonal to lines joining pod-mounted target pairs and in the plane of this ring of targets (or a circle fitted through this ring of targets) provide an estimate of the instantaneous position of the center of the hub, thereby providing a basis for estimating more accurately the location of the blade relative to the hub and rotor shaft. However, the initial results presented in this report will only use the first approach described above.

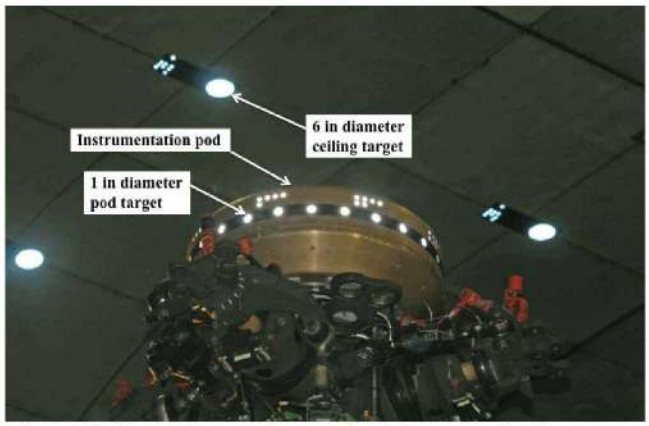

Figure 7. Instrumentation pod with one-inch diameter retro reflective targets installed.

The data reduction software consists of a suite of Matlab functions that have been custom designed at NASA for image processing and photogrammetric analysis of rotor system image sequences. A small subset of functions for image processing, photogrammetry, and coordinate transformations, taken from a Matlab toolbox developed by Western Michigan University for NASA (Ref. 8) are integrated within this rotor-specific suite of functions. With the exception of some image quality assessments, analysis of IBC data has been performed post test at sites remote from the NFAC. Although a limited amount of automation has been implemented in the Matlab data reduction functions, it is likely that for the near future (e.g., Airloads testing) significant amounts of post-test processing will be needed even for the initial image processing. The main reason for this is the extreme variation in the brightness of the blade targets as a function of blade azimuth, camera position (including physical constraints on allowable camera locations), and rotor operating condition that can occur during testing. Such large variations in contrast currently require some user intervention for only the first image of each image sequence. After the target locations in the camera CCD pixel coordinate system for the one image are successfully determined, full automation is generally possible for the rest of the image sequence. Note that this user intervention is needed to initiate image sequence processing for each camera.

After image sequences are processed to find the locations of targets along the blade for at least two cameras, photogrammetric intersection is used to determine the 3D coordinates of the targets in the wind-tunnel coordinate system. Prior to photogrammetric intersection, camera calibrations are used to correct each image for significant distortion caused by the wide angle camera lenses that are necessary to view an entire blade anywhere in the quadrant of interest. The position of a blade in the rotor system is determined as follows. Target coordinates in the wind-tunnel system are first transformed about the cross-stream axis to account for shaft angle of attack. The blade position is then determined by nonlinear least squares fitting the target coordinates in the tunnel system to reference blade target coordinates (measured using the GSI photogrammetric measurement system) established at zero azimuth in the wind-tunnel XYZ-coordinate system. Considering the 3 Euler angles found from this transformation, blade pitch will then be proportional to the angle about the X-axis, blade flap will be proportional to the angle about the Y-axis, and lead-lag will be proportional to the difference between the angle about the Z-axis minus the azimuth of the hub as measured by the NFAC rotor shaft encoder. The generalized extraction of elastic bending and torsion from these types of data sets is particularly challenging and has not been fully implemented to date. Several methods are being investigated in order to find a suitable approach.

RESULTS

Spatial Mapping of Rotor Blade Retro-Reflective Targets

Fifty 2-inch diameter retro-reflective targets were applied to the lower surface of rotor blades number 1 and number 2. The target spatial locations were measured with an average standard deviation of better than 0.001 inch using the previously mentioned GSI V-STARS photogrammetric measurement system. The target locations were measured with the blades lying in an unloaded horizontal position, lower surface up and supported intermittently along the span of the blade (see Fig. 5). In order to reference the blade targets to the rotor and airfoil system geometry, additional retro-reflective targets were placed at the blade-to-spindle-attachment boltholes and the blade trailing edge during the V-STARS measurement. Mapping the location of the two 1-inch diameter blade-to-spindle-attachment bolt holes provided a measurement of the radial location of each target and a reference chordline defining zero static twist of each blade. Collectively this data provides the basis for computing, at each radial station, the location and orientation of the blade sectional chordline from the photogrammetric measurement of these blade-surface-mounted targets in the wind-tunnel coordinate system. This estimation from measured surface target locations of the blade sectional chordline is dependent on the assumption that the as-built airfoil contours at each measurement station of each rotor blade are per Ref. 9 blade geometry data.

Figure 8 compares the measured twist distribution with the as-designed built-in twist distribution (Ref 10) using the coordinate transformation and sectional chordline estimation detailed above. Since there are three retro-reflective targets at each radial location, there are also three independent estimates of twist. The slight scatter in the twist values at each radial location is possibly due to airfoil lower-surface contours not matching the as-designed geometry. On average, the estimated twist is offset below the as-designed blade twist by about 0.25 deg. Also, had these measurements been made with the blade supported vertically (thus lessening the effect of blade weight), this difference would be expected to increase slightly in the outboard portion of the blade.

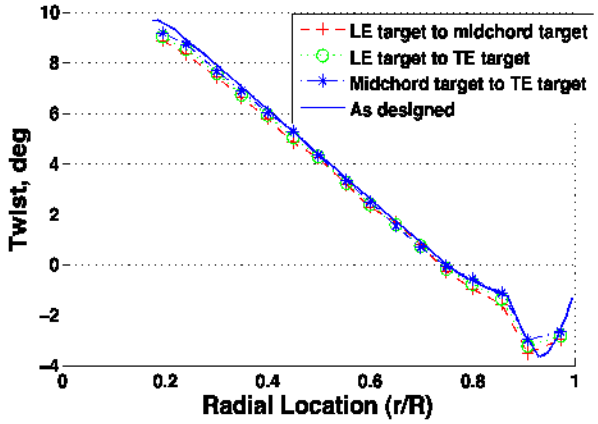

Figure 8. Built-in twist distribution of blade number 2, comparison of as-designed to as-measured using surface mounted retro-reflective targets.

Image Quality

The quality of images acquired during forward flight testing was assessed for each camera pair by determining the number of common targets identified during the target centroiding process. In addition, combining the IBC image analysis with an analytical analysis allowed for an assessment of camera locations with the goal of improving image quality for the planned 2010 UH-60 Airloads test.

Determining target location in XYZ-space requires the target be centroidable in each of the simultaneous images captured by that quadrant's camera pair. Accurate measurement of blade deflections at an instant in time expands this requirement to the set of targets distributed along the span of the blade. For this experiment, the minimum acceptable number of common centroidable targets, for measuring blade deflections, might be 20 of the 50 blade targets. Figure 9, shows two sets of image pairs where the contrast of each image has been adjusted such that the retro-reflective blade and ceiling targets illuminate with little or no background interference from the rest of the image. Figure 9 (a) is a quadrant I image pair, from cameras 1 and 2, with blade 1 at 45 deg azimuth. This is a case where the image quality is quite high and all targets were clearly visible and centroidable. Thus, for this condition, the image pair produced 50 centroidable targets. Figure 9 (b) is a quadrant IV image pair, from cameras 7 and 8, with blade 2 at 345 deg azimuth. The image from camera 8 produced 50 centroidable targets. In contrast to camera 8, the image quality for camera 7 is marginal, particularly at the inboard section of the blade, resulting in only 21 centroidable targets.

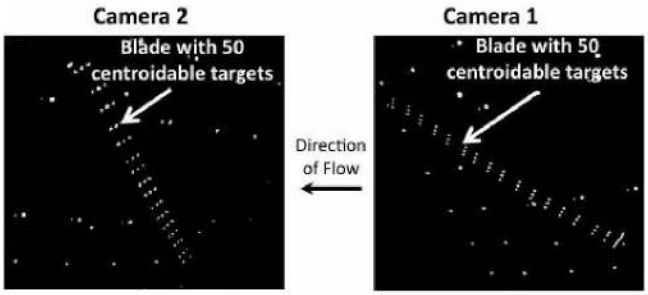

(a) Quadrant 1 Camera Pair, α_s = 0 deg, μ = 0.15, blade azimuth = 45 deg

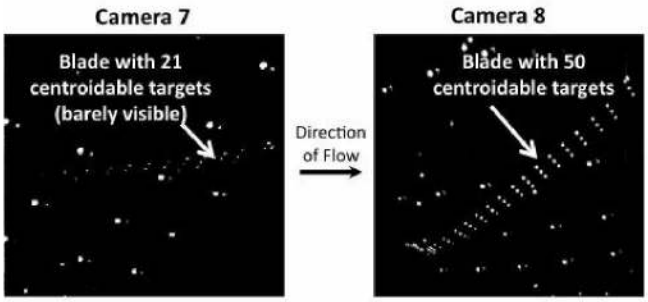

(b) Quadrant 4 Camera Pair, α_s = -7.6 deg, μ = 0.35, blade azimuth = 345 deg

Figure 9. Image quality assessment under forward flight test conditions.

The primary factor affecting the signal strength from difficult-to-see targets is the oblique angle at which the targets are viewed. As shown in figure 3, camera 7 views the blade in quadrant IV from the trailing edge side of the blade. For this view, the angle of attack, positive twist at the inboard section of the blade, positive collective angle (11.5 deg), and positive cyclic angle (longitudinal cyclic of 7.8 deg), all contribute to the increased angle of incidence to the blade's targets. In addition, the relatively large straight-line distance between the camera and the blade exacerbates the low target intensity. As the blade continues to rotate beyond 345 deg azimuth, target visibility from camera 7 continues to decrease.

Based on the experimental results obtained to date and numerical simulation of the experiment, quadrant IV at azimuthal locations near 330 deg and beyond with the model at high negative shaft angle and high collective is anticipated to be the most difficult combination of operating conditions and blade location for obtaining high quality images. Image sets obtained during IBC were combined with analytical simulations of the quality of image pairs to assess camera locations that would enhance image pair quality during 2010 Airloads testing. The simulation captures the rotor disk and provides estimates of two important measures of image quality, light intensity returned from the targets and target size (in pixels) on the camera CCD. The analysis includes the effect of shaft angle, collective, lateral and longitudinal cyclic, built in twist, elastic twist, blade flap, chordwise location of the targets on the local airfoil section, and extreme sensitivity of retro-reflective target signal return to viewing angle. The simulation assumes the strobe light is spherically uniform, emanating from the camera location. Simulations of individual camera image quality are combined to provide an evaluation of the integrated performance of a camera pair.

The simulations provided a predicted luminosity value throughout the quadrant of interest for each camera. Results from camera pairs were combined to provide an evaluation of the integrated luminosity for that pair of cameras in the specified quadrant. Figure 10 illustrates the effect of camera location on camera pair performance as predicted by the minimum signal strength between the two cameras for each location on the rotor disc. Figure 10 (a) illustrates the results for the camera 7 and 8 pairing in quadrant IV. Since the blade rotates away from camera 7 in a high leading-edge-up attitude, this camera dominates the combined camera performance. Therefore, the combined camera performance shows weak target luminosity throughout most of the quadrant.

Alternate camera locations were assessed to improve luminosity performance in quadrant IV (Fig. 10b). Cameras 7 and 8 were shifted downstream and camera 8 was pushed out onto the test-section floor, resulting in an overall improvement in image quality. In addition, this new camera 8 location permits intersection with simultaneous images

obtained from camera 1 that should result in high quality image pairs near 360 deg azimuth.

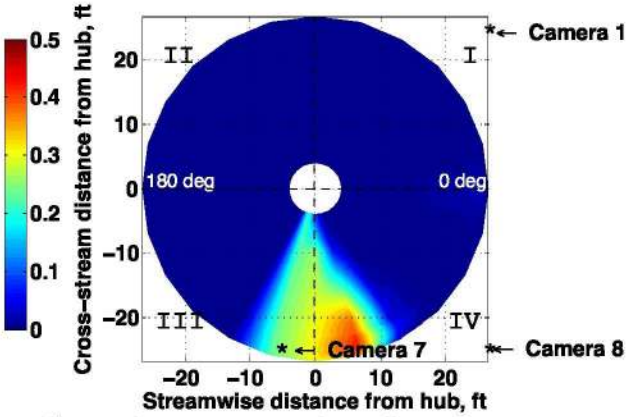

(a) Quadrant IV cameras located per IBC test set up

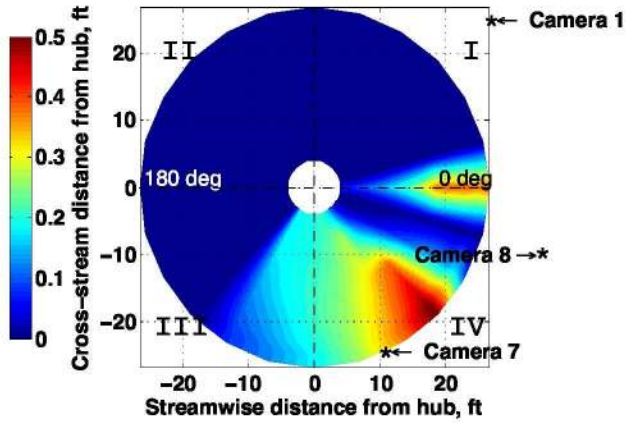

(b) Quadrant IV camera set up for planned Airloads test

Figure 10. Effect of camera location on quadrant IV image quality. Color contours are target luminosity normalized by the brightest target viewed by either camera of a camera pair. Airflow is from left to right.

This analysis was applied to all 8 cameras and all camera pairs with overlapping views of the rotor disk. These analyses were conducted for a range of candidate Airloads test conditions to help insure that the cameras would provide quality images across the anticipated Airloads test matrix. Figure 11 shows the camera locations selected for Airloads testing. Note that two of the cameras, one in quadrant II and one in quadrant IV, are located out on the test-section floor. The overall effectiveness of this combination of camera locations on target illumination is illustrated in Fig. 12 for test conditions comparable to the Airloads flight test counter C8534. The most difficult azimuths to get very high quality images pairs will be in the vicinity of 345 deg. Nevertheless, experience gained through processing of images from the IBC test indicates that camera-location and other adjustments (Ref. 11) will significantly improve the probability of success in this azimuthal area across most of the span of a blade, even at difficult test conditions like C8534. Additional avenues for improving image quality include increasing the number of strobes per camera and/or directing more of the available light in areas where the target signal is weak, reducing the light loss from the windows by using low-reflectance glass, keeping the targets clear of dust and oil contamination by careful handling and occasional cleaning during testing, and the possible use of an alternate retro reflective material with a higher return signal at high angles of light incidence.

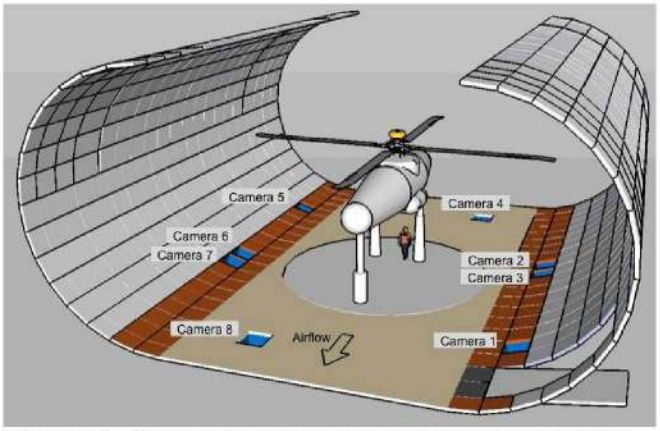

Figure 11. Camera locations selected for planned 2010 Airloads test.

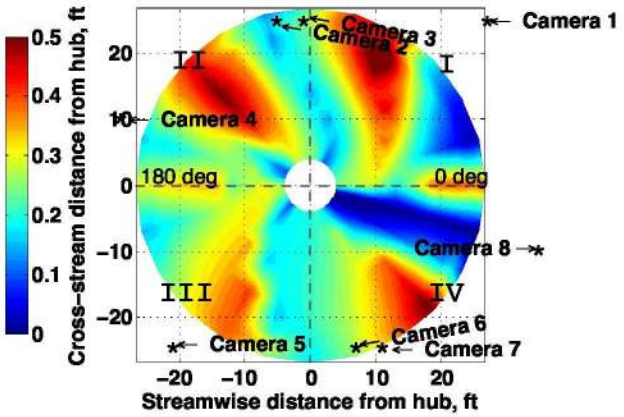

Figure 12. Assessment of target illumination for camera locations selected for the planned 2010 Airloads wind-tunnel test. Color contours are target luminosity normalized by the brightest target viewed by either camera of a camera pair.

How Much Data Is Enough?

The accuracy of the deflection measurement is, of course, dependent on the range of variation of the particular measurement being sampled and the number of samples acquired. In an effort to assess how much image data is required, for example, to measure blade tip displacement, data from the 2003 full-scale UH-60 wide-chord blade rotor system test (Ref. 12) in the NASA Ames 40- by 80-Foot Wind Tunnel is used as illustrated below.

Motion of the tip of the blade in the flapping direction is the extreme case in terms of maximum anticipated blade elastic deflection. Blade tip displacement is dependent on rotor operating conditions such as advance ratio, thrust and the azimuthal position of the blade. The 2003 UH-60 blade

flapping measurements were obtained using the same blade motion hardware (BMH) measurement system (Ref. 13 and Ref. 14) used during the UH-60 Airloads flight test (Ref. 1). The data used below was obtained at an advance ratio of 0.35 (V = 150 kts) with a thrust (C_T/σ) of 0.082, α_S = -5.0 deg, collective = 10.7 deg, lateral cyclic = 1.6 deg and longitudinal cyclic = 7.0 deg. The blade tip motion in the flapping direction is estimated by assuming the blade flaps as a solid body. Blade 3, selected for this study, was not one-per-rev trimmed. The 256 revs of data are shown in Fig. 13.

An assessment of the ability of an ensemble average to predict mean blade deflections, as a function of azimuth, is also shown in Fig. 13. At Ψ = 220 deg, where the rev-to-rev variations are the largest, an ensemble average of 30 measurements will, with a certainty of 95%, be within 0.45 inches of the true mean (shown as error bar or max error curve). By comparison, at Ψ = 60 deg where the rev-to-rev variations are small an ensemble average of 30 measurements will, with a certainty of 95%, be within 0.15 inches of the true mean.

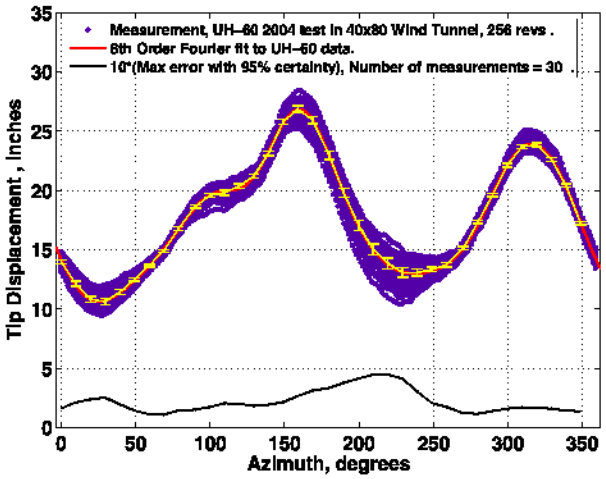

Figure 13. Assessment of the rev-to-rev and azimuthal variation in tip location based on non-stereo-photogrammetry measurements. Maximum error with 95% certainty, based on 30 measurements, is also shown as error bars.

Using the 2003 UH-60 measurements, the blade tip-displacement Fourier modes were estimated and are shown in Fig. 14. The amplitude of the 6th mode is 0.30 inches indicating that a 30-revolution ensemble average will, at best, provide reasonable mode information out to the 5th mode. To capture the 6th and possibly the 7th modes would require the number of revs of data be increased by at least a factor of 10, to roughly 300 revs of data at each azimuth. To capture the 7th mode could also require photogrammetry data be acquired at 10-degree or 12-degree azimuthal increments. For example, during the IBC test, a typical data set was every 15 deg with 15-images sets acquired at each of azimuth. However, in some instances as many as 200 image sets were obtained. Furthermore, in few test runs, blade displacement measurements were acquired at azimuthal increments of 10 deg.

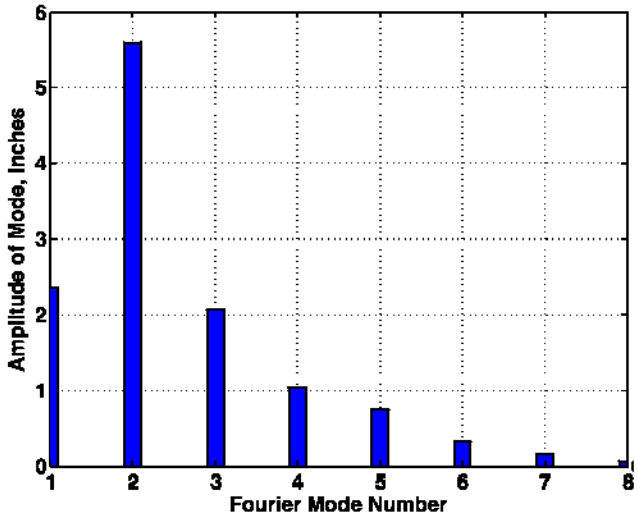

Figure 14. Estimated Fourier mode blade tip displacement amplitude based on measurements obtained during 2004 test of a UH-60 rotor system in the NFAC.

It is currently planned that during Airloads testing, the standard azimuthal increment will be 15 deg at 30 images sets per azimuth. For particularly interesting or unusual test conditions the number of image sets per azimuth can be increased to several hundred. For portions of the test matrix where acquiring data quickly over a range of test conditions is the priority, the number of image sets per data point will be reduced to 15, or possibly fewer.

EXAMPLES OF MEASUREMENTS OBTAINED DURING IBC TESTING

An example of measurements made during the IBC test, Fig. 15, shows the measured radial pitch distribution of blade 1 at 40 deg azimuth. Fifteen revolutions of superimposed data indicate that at this azimuth and test condition the rev-to-rev variation in pitch distribution (includes elastic twist) is relatively small.

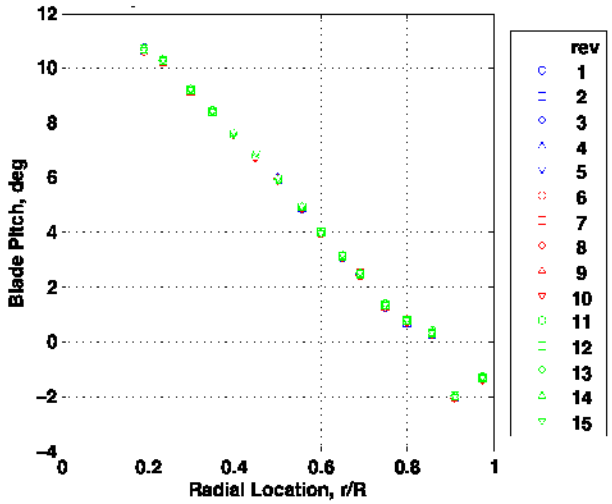

Figure 15. Measured pitch distribution μ=0.20, α_S = -1.6 deg, C_T/σ = 0.078, collective = 6.7 deg, Ψ = 40 deg.

One of the more difficult measurements to make accurately is the elastic twist distribution of a blade. This measurement utilizes the three relatively closely spaced targets to obtain three separate measurements at each radial position. For each test condition and azimuthal location ensemble averages, typically 15 images sets for the IBC test, then provide three measures of local airfoil-section blade pitch. The rigid as-measured built-in twist is subtracted from the measured sectional blade pitch at each radial station to yield an estimate of the blade elastic twist distribution. The average of these three, at an azimuth of 40 deg, is shown for the 16 spanwise stations in Fig. 16. This data was obtained at an advance ratio of 0.20 and C_T/σ of 0.078. The measured twist distribution across the span is not as "smooth" as expected, possibly due in part to the previously mentioned possibility that the lower surface of the blade does not match the as-design shape with the necessary accuracy. For example a difference between the as-built and as-designed shapes in the normal-to-chord direction of 0.015 inches could result in differences ranging from 0.1 to 0.2 deg in photogrammetrically measured blade pitch or elastic twist.

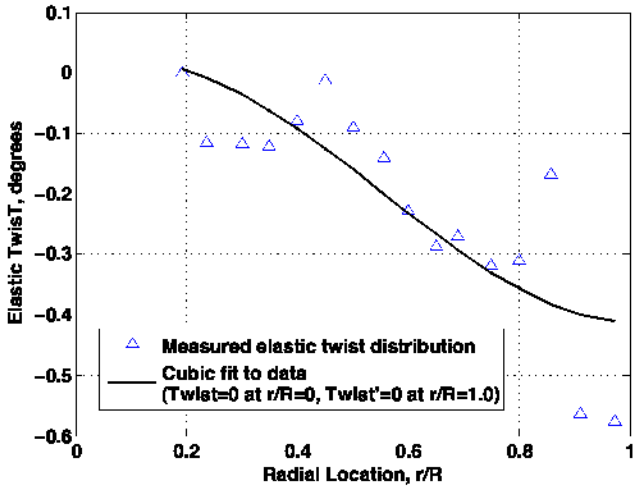

Figure 16. Elastic twist of blade 1, C_T/σ=0.078, μ=0.20, α_S=-1.6 deg, q=24.8 lb/ft^2, Ψ = 40 deg.

For the same test conditions, the photogrammetrically measured blade pitch at r/R = 0.2 was compared to that computed using the UH-60A/LRTA control system settings using either the as-designed or the as-measured built-in twist. The differences, photogrammetrically measured minus computed, are -0.44 deg and 0.27 deg respectively.

During the IBC forward-flight testing, measurements of individual blade-root pitch, flap and lag were made using the BMS measurement system. Blade-root flap was also estimated using the BD system by determining the rotation of the blade required to least-square fit the stereo image measured target locations to the target locations as measured statically by the GSI system. For this fit the inner 25% of the available targets were used. Comparison of measurements from these two methods are shown in Fig. 17 for two test conditions, rotor trimmed from 270 to 90 deg azimuth and rotor untrimmed at Ψ = 0 deg. The data show a relatively consistent offset between the two measurement methods of about 0.5 deg. Due to deteriorating image quality and subsequent "loss" of targets, particularly on the inboard portion of the blade, as the blade moved from 315 to 360 deg azimuth, the photogrammetrically derived flap measurement becomes increasingly suspect. Nevertheless, the level of agreement is encouraging and it is probable that with higher quality images and improvements in image processing techniques better agreement can be achieved. It is of interest to note that the measured trim-induced change in flap at Ψ = 0 from the two measurement techniques are in good agreement, -2.4 deg.

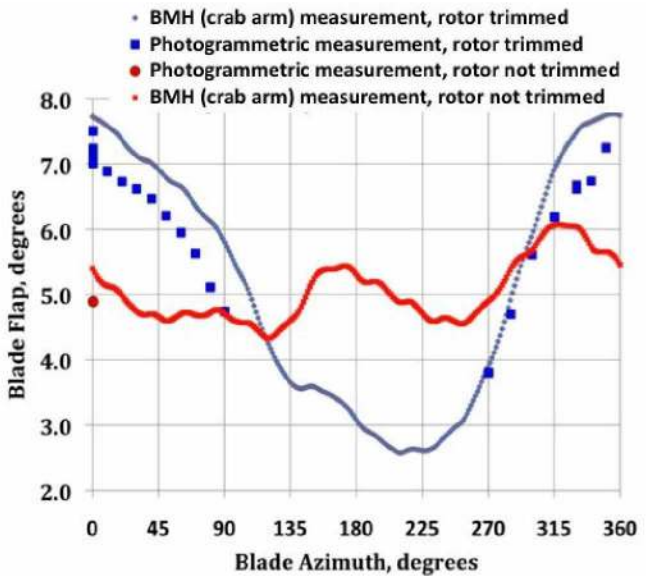

Figure 17. Comparison of measured blade flap of blade 1, C_T/σ=0.078, μ=0.25, α_s=-3.0 deg, q=7.8 lb/ft^2.

CONCLUSIONS

The ability to photogrammetrically measure blade deflection of a full-scale UH-60 rotor during wind-tunnel testing at conditions representative of actual free-flight conditions has been successfully demonstrated. Sufficient experimental data was obtained in quadrants I and IV so that, combined with simulations of the measurement system, configuring an improved stereo photogrammetry system is expected. This system will enable the acquisition of blade elastic displacement data sets for future aeromechanics analysis development and validation. A four-quadrant stereo photogrammetry system is expected to be fully operational during the planned 2010 Airloads wind-tunnel test.

ACKNOWLEDGMENTS

Many thanks to Harriett Dismond, NASA Langley Research Center and Eduardo Solis, Monterey Technologies Inc. for their dedicated support. Thanks also to Dr. Alan Wadcock for his invaluable technical insights and advice throughout this effort. This work was supported by the NASA Subsonic Rotary Wing Project.

REFERENCES

[1]Kufeld, R. M., D. L. Balough, J. L. Cross, K. F. Studebaker, C. D. Jennison, and W. G. Bousman, "Flight Testing the UH–60A Airloads Aircraft." Proceedings of the 50th Annual Forum of the American Helicopter Society, Washington, D.C., May 1994.

[2]Schneider, Oliver, and van der Wall, Berend G., "Final Analysis of HART II Blade Deflection Measurement," 29th European Rotorcraft Forum, Friedrichshafen, Germany, September 16-18, 2003.

[3]Barrows, Danny, "Blade Deformation System Demonstration in NFAC," NASA Fundamental Aeronautics 2008 Annual Meeting, Atlanta, GA, October 7-9, 2008.

[4]Amer, T. R. and Goad, W. K., "WingViewer: Data-Acquisition Software for PSP/TSP Wind-Tunnel Cameras," NASA Langley Research Center, LAR-16474-1, Oct 2005.

[5]Fleming, G. A., "RASP: Rotor Azimuth Synchronization Program (RASP) User's Guide, Version 1.3," NASA Langley Research Center, February 6, 2008.

[6]Burner, A. W.; Radeztsky, R. H.; Liu, T.: "Videometric Applications in Wind Tunnels," presented at the SPIE International Symposium on Optical Science, Engineering, and Instrumentation, Videometrics V, 30-31 July 1997, SPIE vol. 3174 pp. 234-247.

[7]Brown, J., "V-STARS/S Acceptance Results," Boeing Large Scale Optical Metrology Seminar, Seattle, WA, 1998.

[8]Liu, T. and Burner, A. W., "Photogrammetry Toolbox User's Guide," Western Michigan University, May 2007.

[9]Bousman, W. G., "Aerodynamic Characteristics of SC1095 and SC1094R8 Airfoils," NASA TP–2003-212265, AFDD/TR-04-003.

[10]Arcidiacono, Peter and Zincone, Robert, "Titanium UTTAS Main Rotor Blade", Proceedings of the 31st Annual National Forum of the American Helicopter Society, Washington, D.C., May 1975.

[11]Barrows, Danny, and Abrego, Anita, "Blade Deflection Measurement Developments for Airloads Testing", NASA 2009 Fundamental Aeronautics Program Annual Meeting, September 29 – October 1, 2009.

[12]Shinoda, P. M., Norman, T. R., Jacklin, S. A., Yeo, H., Bernhard, A. P. F., and Haber, A., "Investigation of a Full-Scale Wide Chord Blade Rotor System in the NASA Ames 40- by 80-Foot Wind Tunnel", American Helicopter Society 4th Decennial Specialist's Conference on Aeromechanics, San Francisco, CA, January 21-23, 2004.

[13]Balough, D. L., "Estimation of Rotor Flapping Response Using Blade-Mounted Accelerometers", American Helicopter Society Aeromechanics Specialists Conference, San Francisco, California, January 19-21, 1994.

[14]Gagnon, R., "Blade Motion Sensor System Calibration," United Technologies Sikorsky Aircraft SER-70486, October 1981.